

A Semi-analytical Solution for Time-variant Thermoelastic Creep Analysis of Functionally Graded Rotating Disks with Variable Thickness and Properties

M. T. Ghorbani*

Department of Mechanical Engineering,
University of Kashan, Kashan, Iran
Email: m.ghorbani.ph@gmail.com

*Corresponding author

Received 14 November 2011; Revised 29 December 2011; Accepted 26 February 2012

Abstract: A time domain semi-analytical solution to study thermo-elastic creep behaviour of functionally graded rotating axi-symmetric disks with variable thickness is presented. The rate type governing differential equations for the considered structure are derived and analytically solved. To solve these equations, the disk is divided into virtual sub-domains. General solution of equilibrium equations in each sub-domain can be obtained by imposing the continuity conditions at the interface of the adjacent sub-domains together with global conditions. Finally, the solution in terms of rate of stress and strain is obtained. The advantage of the present work is to avoid simplifications and restrictions, which are normally associated with other creep solution techniques in the literature. Results for the stress and strain rates of the disk subjected to centrifugal forces and thermal loadings for different boundary conditions are presented. Results obtained are verified with those available in the literature for easier cases.

Keywords: Functionally Graded Materials, Norton's law, Semi Analytical Method, Steady State Creep, Variable Thickness

Reference: M. T. Ghorbani (2012) 'A Semi-analytical Solution for Time-variant Thermo-elastic Creep Analysis of Functionally Graded Rotating Disks with Variable Thickness and Properties', *Int. J. Advanced Design and Manufacturing Technology*, Vol. 5/ No. 2, pp. 41-50

Biographical notes: **M. T. Ghorbani** received his B.Sc. in Mechanical Engineering from University of Kashan 2010. He is currently Engineer at Armaghan Kavir Company, Kashan, Iran. His current research interest includes Stress Analysis of FGM Disks and Cylinders.

1 INTRODUCTION

In recent years with the development of powerful engines, turbines, reactors and other machines the need for materials with high thermal and mechanical resistance has been felt. In former years, pure ceramic materials for coating components, used in high temperature environments, were used. These materials were very good insulators, but did not have enough resistance against the residual stress. Residual stresses in these materials are troublesome, including holes and cracks. Later, in order to eliminate these problems, laminated composite materials were used. But thermal stress caused the lamination phenomenon in these materials. Due to these problems, material engineers in 1984 in Sendai in Japan suggested functionally graded materials (FGM) with high thermal resistance [1].

FGMs are composite materials with heterogeneous microstructure whose mechanical properties vary continuously and have specified material property variations. The most common type of FGM is composed of metal and ceramic. These materials are obtained from mixing metal powder and ceramic. Variation of metal and ceramic is completely continuous so that one surface is pure ceramic material, and the other is a pure metal surface. Between the two surfaces composition is continuous. These materials have better effective mechanical properties than laminated composites.

To obtain the basic and fundamental results in most cases, the stress in plates, disks and cylinders have been investigated. Yang in 1999 [1], provided an analytical solution for creep behaviour of elastic cylinders made of FG materials which are just under thermal load. This solution can be used to study the dependence of stress to temperature and time for FG structures. He assumed that the Poisson ratio and material constants in Norton's principle, which vary along the cylinder radius, are constant values. Finally, the analytical results were compared with FEM. Singh and Ray in 2002 [2], presented stable creep analysis of anisotropic rotating disk made of composite materials, including silicon carbide particles in the pure aluminium matrix using Hill's yield criterion. His results were compared with that of Von mises yield criterion for isotropic composite.

K. M. Liew and his colleagues in 2003 [3], provided a semi-analytical method for thermo-elastic behaviour of hollow cylinders made of FG material. They divided the cylinder along its radius and assumed each division to have homogeneous properties. They finally, simplified equations and solved them. S. B. Singh and

S. Ray in 2003 [4], investigated creep behaviour of rotating disk made of FG materials. Their studied disk was made of a composite, including silicon carbide particles in a pure aluminium matrix. They explained steady state creep behaviour using Norton's principles. They showed that in the rotating isotropic disk, assuming linear particle distribution, radial and tangential creep rate is smaller than the disc with uniform particle distribution.

Islami and colleagues in [5], presented a one-dimensional analytical solution method for mechanical and thermal stress of thick hollow FG spheres. They assumed that thermal distribution is a function of radius. Moreover, they assumed that material properties, except for Poisson's ratio, vary along the radius according to Power-law function.

Kordkheili and Naghdabadi [6], presented a semi-analytical thermo-elastic solution for hollow and solid rotating axi-symmetric disks made of functionally graded materials under plane stress conditions. They divided their studied disc along the radius and assumed that material properties in each division were constant. With this method, they could solve ODEs obtained for analysis of displacement and temperature easily. Farshi and Bidabadi in 2008 [7], presented a method for optimizing the thickness distribution of Heterogeneous rotating disk, in order to minimize its weight. They controlled secondary creep amount in the disk so that stress in the disk didn't exceed a permissible limit.

Singh in 2008 [8], offered an analytical method for steady state creep behaviour of rotating discs made of anisotropic composite materials, including silicon carbide particles in the aluminium matrix using Norton's principle. He calculated distribution of stress and strain rate for the anisotropic disk and compared it with the isotropic disk. Poultangari and his colleagues in 2008 [9], presented an analytical method that can be used to obtain mechanical and thermal stress responses of two-dimensional steady state in a thick hollow sphere made of FGMs. They assumed that material properties vary along the radius according to Power Law and achieved thermal distribution by solving the energy equation for FGMs.

Pankaj, and Sonia R. Bansal in 2008 [10], achieved stress and creep strain rates for thin rotary disk with variable density using Seth's transition theory. Bayat and colleagues in 2009 [11], calculated mechanical and thermal stress in rotating variable thickness discs made of FGMs under constant temperature and radial axi-symmetric load. In the present article, time-dependent creep stress analysis of rotating thin disk made of FG materials will be examined. To examine the effect of

basic and important factors such as the gradual change of thermo-mechanical properties, centrifugal force and thermal load on the stress, creep rate and disk displacement of axi-symmetric rotating disk made of FGM, a precise method has been proposed. Using the desired method provides the possibility to solve the governing equations without any need to assume some properties and variable coefficients to be constant, also there will be no need to consider the derivative terms of variable parameters in the governing equations to be constant. Other advantages of this method are that changes in material properties and temperature along the disk radius are considered carefully.

Equilibrium equations based on thermo-elastic theory for rotating FG disks are inferred and using them the displacement equation is derived. To obtain thermal distribution in the disk, nonlinear heat transfer equation along the radius is used. Also, using Norton's principle, steady state creep equation for the disk is inferred. To solve the mentioned equations, the radial domain of the disk is divided into virtual sub-domains where, in each sub-domain, the thermo-mechanical property is assumed to be constant. This assumption yields the governing equilibrium equations in each sub-domain as ordinary differential equations with constant coefficients whose general solution can be written involving certain unknowns. These unknowns can be determined as solution of the system of linear algebraic equations obtained by imposing the continuity conditions at the interface of the adjacent sub-domains together with global conditions. Using the response of heat transfer equation, thermal distribution in each sub-domain and thus thermal distribution in the total disk is achieved. Inserting the thermal distribution in the displacement equation, displacement, stress and strain in each sub-domain, and finally in the total disk arise.

2 GRADATION RELATION

Consider a thin hollow axi-symmetric FG disk with variable thickness with inner radius r_1 and outer radius r_0 , as shown in Fig. 1. The disk rotates at an angular velocity ω and is subjected to thermal loading $\Delta T(r)$ from steady state condition. The problem is assumed to be plane stress. Due to axial symmetry assumptions in geometry and loading, cylindrical coordinate system (r, θ, z) is used. The inner and outer surfaces of the FG disk are assumed to be metal-rich and ceramic-rich, respectively. Between these two surfaces material properties vary according to Eq. (1).

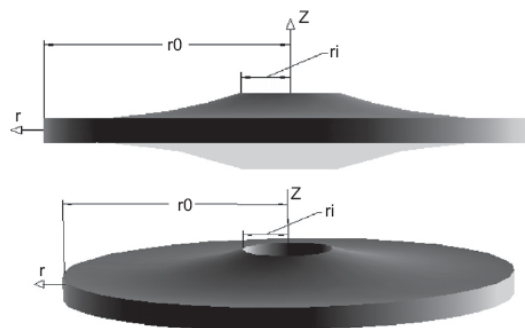


Fig. 1 Configuration of the thin-walled FG rotating disk [11]

The most common model for expressing the variation of material properties in FGMs is the power-law distribution of the volume fraction. Based on this model, the material property gradation through the disk radius is represented in terms of the volume fraction by:

$$P(r) = (P_0 - P_1) \left(\frac{r - r_1}{r_0 - r_1} \right)^n + P_1 \quad R_i \leq r \leq R_o \quad (1)$$

where $p(r)$ denotes a generic material property and P_0 and P_1 denote the property of the outer and inner faces of the disk, respectively (e.g. elastic modulus) and n is a grading index that dictates the material variation profile through the thickness. This study assumes that the elastic modulus E , thermal coefficient of expansion α , density ρ and heat conductivity K and the Poisson's ratio ν vary according to the gradation Eq. (1).

3 CREEP EQUATIONS IN FG DISKS

Strain rate for radial and tangential direction of rotating disks are [7]:

$$\dot{\epsilon}_{rr} = \frac{d\dot{u}}{dr}, \dot{\epsilon}_{\theta\theta} = \frac{\dot{u}}{r} \quad (2)$$

$$\begin{cases} \dot{\epsilon}_{rr} = \dot{\epsilon}_{rr,T} + \dot{\epsilon}_{rr,c} = \frac{1}{E} (\dot{\sigma}_{rr} - \nu(r)\dot{\sigma}_{\theta\theta}) + \dot{\epsilon}_{rr,c} \end{cases} \quad (3)$$

$$\begin{cases} \dot{\epsilon}_{\theta\theta} = \dot{\epsilon}_{\theta\theta,T} + \dot{\epsilon}_{\theta\theta,c} = \frac{1}{E} (\dot{\sigma}_{\theta\theta} - \nu(r)\dot{\sigma}_{rr}) + \dot{\epsilon}_{\theta\theta,c} \end{cases} \quad (4)$$

Here $\dot{\epsilon}_{rr}, \dot{\epsilon}_{\theta\theta}$ are radial and tangential strain rate respectively and $\dot{\epsilon}_{rr,T}, \dot{\epsilon}_{\theta\theta,T}$ denote radial and tangential strain rate due to thermal load and $\dot{\epsilon}_{rr,c}, \dot{\epsilon}_{\theta\theta,c}$ denote radial and tangential creep strain rate. In time hardening theory, creep strain rate is [1]:

$$\dot{\epsilon}_{rr,c} = \frac{\kappa \sigma_{eff}^{\xi-1}}{2q} (2\sigma_{rr} - \sigma_{\theta\theta}) \tau^{q-1} \quad (5)$$

$$\dot{\epsilon}_{\theta\theta,c} = \frac{\kappa \sigma_{eff}^{\xi-1}}{2q} (2\sigma_{\theta\theta} - \sigma_{rr}) \tau^{q-1} \quad (6)$$

Here κ, ξ are creep constants also τ is creep time and q is constant. σ_{eff} equals to:

$$\sigma_{eff} = \sqrt{\sigma_{rr}^2 - (\sigma_{rr} \times \sigma_{\theta\theta}) + \sigma_{\theta\theta}^2} \quad (7)$$

Radial and tangential stress rate with plane stress condition are according to Eq. (8), (9).

$$\dot{\sigma}_{rr} = \frac{E(r)}{1-\nu^2} (\dot{\epsilon}_{rr} + \nu(r)\dot{\epsilon}_{\theta\theta} - (\dot{\epsilon}_{rr,c} + \nu(r)\dot{\epsilon}_{\theta\theta,c})) \quad (8)$$

$$\dot{\sigma}_{\theta\theta} = \frac{E(r)}{1-\nu^2} (\nu(r)\dot{\epsilon}_{rr} + \dot{\epsilon}_{\theta\theta} - (\nu(r)\dot{\epsilon}_{rr,c} + \dot{\epsilon}_{\theta\theta,c})) \quad (9)$$

Equilibrium equation for stress rate of a rotating disk with angular velocity of ω and thickness of $h(r)$ is [7]:

$$\frac{d}{dr} (h(r)r\dot{\sigma}_{rr}) - h(r)\dot{\sigma}_{\theta\theta} + h(r)\rho(r)\omega^2 r^2 = 0 \quad (10)$$

where $\dot{\sigma}_{rr}, \dot{\sigma}_{\theta\theta}$ is radial and tangential stress rate respectively.

Using Eq. (2) and substituting it in Eq. (8), (9) and substituting achieved equations in Eq. (10) we have Creep behaviour equation of FG disks (Eq. (11)).

$$\left[\frac{E(r)}{1-\nu(r)^2} \right] \frac{d^2 \dot{u}}{dr^2} + \left[\frac{1}{h(r)} \frac{dh(r)}{dr} \left(\frac{E(r)}{1-\nu(r)^2} \right) + \frac{\nu(r)}{r} \left(\frac{E(r)}{1-\nu(r)^2} \right) + \frac{1}{r} \left(\frac{E(r)}{1+\nu(r)} \right) + \frac{d}{dr} \left(\frac{E(r)}{1-\nu(r)^2} \right) \right] \frac{d\dot{u}}{dr} + \left[\frac{\nu(r)}{r^2} \left(\frac{E(r)}{1-\nu(r)^2} \right) - \frac{1}{r^2} \left(\frac{E(r)}{1+\nu(r)} \right) + \frac{\nu(r)}{r} \frac{d}{dr} \left(\frac{E(r)}{1-\nu(r)^2} \right) + \frac{1}{r} \frac{d\nu(r)}{dr} \left(\frac{E(r)}{1-\nu(r)^2} \right) - \frac{1}{r} \left(\frac{E(r)}{1+\nu(r)} \right) - \frac{d}{dr} \left(\frac{E(r)}{1-\nu(r)^2} \right) + \frac{\nu(r)}{h(r)} \frac{dh(r)}{dr} \left(\frac{E(r)}{1-\nu(r)^2} \right) + \frac{1}{r} \left(\frac{E(r)}{1+\nu(r)} \right) - \nu(r) \frac{d}{dr} \left(\frac{E(r)}{1-\nu(r)^2} \right) - \nu(r) \left(\frac{E(r)}{1-\nu(r)^2} \right) \frac{d\dot{\epsilon}_{rr,c}}{dr} - \left[\left(\frac{E(r)}{1-\nu(r)^2} \right) \right] \frac{d\dot{\epsilon}_{\theta\theta,c}}{dr} \right] \dot{u} + \left[\frac{1}{h(r)} \frac{dh(r)}{dr} \left(\frac{E(r)}{1-\nu(r)^2} \right) + \frac{\nu(r)}{r} \left(\frac{E(r)}{1-\nu(r)^2} \right) + \frac{1}{r} \left(\frac{E(r)}{1+\nu(r)} \right) + \frac{d}{dr} \left(\frac{E(r)}{1-\nu(r)^2} \right) \right] \dot{\epsilon}_{rr,c} + \left[\frac{\nu(r)}{h(r)} \frac{dh(r)}{dr} \left(\frac{E(r)}{1-\nu(r)^2} \right) + \frac{1}{r} \left(\frac{E(r)}{1+\nu(r)} \right) - \nu(r) \frac{d}{dr} \left(\frac{E(r)}{1-\nu(r)^2} \right) \right] \dot{\epsilon}_{\theta\theta,c} + \left[-\nu(r) \left(\frac{E(r)}{1-\nu(r)^2} \right) \right] \frac{d\dot{\epsilon}_{rr,c}}{dr} - \left[\left(\frac{E(r)}{1-\nu(r)^2} \right) \right] \frac{d\dot{\epsilon}_{\theta\theta,c}}{dr} = 0 \quad (11)$$

$$\left[\frac{\nu(r)}{r} \frac{1}{h(r)} \frac{dh(r)}{dr} \left(\frac{E(r)}{1-\nu(r)^2} \right) - \frac{\nu(r)}{r^2} \left(\frac{E(r)}{1-\nu(r)^2} \right) - \frac{1}{r^2} \left(\frac{E(r)}{1+\nu(r)} \right) + \frac{\nu(r)}{r} \frac{d}{dr} \left(\frac{E(r)}{1-\nu(r)^2} \right) + \frac{1}{r} \frac{d\nu(r)}{dr} \left(\frac{E(r)}{1-\nu(r)^2} \right) \right] \dot{u} + \left[\frac{1}{h(r)} \frac{dh(r)}{dr} \left(\frac{E(r)}{1-\nu(r)^2} \right) + \frac{\nu(r)}{r} \left(\frac{E(r)}{1-\nu(r)^2} \right) + \frac{1}{r} \left(\frac{E(r)}{1+\nu(r)} \right) - \frac{d}{dr} \left(\frac{E(r)}{1-\nu(r)^2} \right) \right] \dot{\epsilon}_{rr,c} + \left[\frac{\nu(r)}{h(r)} \frac{dh(r)}{dr} \left(\frac{E(r)}{1-\nu(r)^2} \right) + \frac{1}{r} \left(\frac{E(r)}{1+\nu(r)} \right) - \nu(r) \frac{d}{dr} \left(\frac{E(r)}{1-\nu(r)^2} \right) \right] \dot{\epsilon}_{\theta\theta,c} + \left[-\nu(r) \left(\frac{E(r)}{1-\nu(r)^2} \right) \right] \frac{d\dot{\epsilon}_{rr,c}}{dr} - \left[\left(\frac{E(r)}{1-\nu(r)^2} \right) \right] \frac{d\dot{\epsilon}_{\theta\theta,c}}{dr} = 0$$

In Eq. (11), the displacement u is only a function of r due to axial symmetry and the plane stress condition.

4 BOUNDARY CONDITIONS

We have 3 kinds of boundary conditions here:

Hollow disk free-free:

$$\dot{\sigma}_{rr} = 0 \text{ at } r = r_i, r = r_o \quad (12)$$

Hollow disk fixed-free:

$$\dot{u} = 0 \text{ at } r = r_i, \dot{\sigma}_{rr} = 0 \text{ at } r = r_o \quad (13)$$

Solid disk:

$$\dot{u} = 0 \text{ at } r = 0, \dot{\sigma}_{rr} = 0 \text{ at } r = r_o \quad (14)$$

5 CREEP SOLUTION: SEMIANALYTICAL SOLUTION

A closed-form solution of Eq. (11) with variable coefficients seems to be difficult. Hence, in this study it

is attempted to find a semi-analytical solution for Eq. (11). In this method, a disk is divided into virtual sub-domains (say m), with t^k denoting the radial-width of the kth sub-domain as shown in Fig. 2. Evaluating the coefficients of Eq. (11) at $r = r^k$, the mean radius of the kth division, an ordinary differential equation with constant coefficients is obtained which is valid in kth sub-domain. That is:

$$(c_1^k \frac{d^2}{dr^2} + c_2^k \frac{d}{dr} + c_3^k) \dot{u}^k + c_4^k = 0 \tag{15}$$

where

$$c_1^k = \left[\frac{E(r^k)}{1 - \nu(r^k)^2} \right] \tag{16}$$

$$c_2^k = \left[\begin{aligned} & \left(\frac{E(r^k)}{1 - \nu(r^k)^2} \right) \times \\ & \frac{1}{h(r^k)} \frac{dh(r)}{dr} \Big|_{r=r^k} \\ & + \frac{\nu(r^k)}{r^k} \left(\frac{E(r^k)}{1 - \nu(r^k)^2} \right) \\ & + \frac{1}{r^k} \left(\frac{E(r^k)}{1 + \nu(r^k)} \right) \\ & + \frac{d}{dr} \left(\frac{E(r)}{1 - \nu(r)^2} \right) \Big|_{r=r^k} \end{aligned} \right] \tag{17}$$

$$c_3^k = \left[\begin{aligned} & \frac{\nu(r^k)}{r^k} \left(\frac{E(r^k)}{1 - \nu(r^k)^2} \right) \frac{1}{h(r^k)} \frac{dh(r)}{dr} \Big|_{r=r^k} \\ & - \frac{\nu(r^k)}{r^{k2}} \left(\frac{E(r^k)}{1 - \nu(r^k)^2} \right) \\ & - \frac{1}{r^{k2}} \left(\frac{E(r^k)}{1 + \nu(r^k)} \right) \\ & + \frac{\nu(r^k)}{r^k} \frac{d}{dr} \left(\frac{E(r)}{1 - \nu(r)^2} \right) \Big|_{r=r^k} \\ & + \frac{1}{r^k} \left(\frac{E(r^k)}{1 - \nu(r^k)^2} \right) \frac{d\nu(r)}{dr} \Big|_{r=r^k} \end{aligned} \right] \tag{18}$$

$$c_4^k = \left[\begin{aligned} & \frac{1}{h(r^k)} \frac{dh(r^k)}{dr} \left(\frac{E(r^k)}{1 - \nu(r^k)^2} \right) \\ & - \left(\frac{E(r^k)}{1 - \nu(r^k)^2} \right) \frac{d\nu(r)}{dr} \Big|_{r=r^k} \\ & - \frac{1}{r^k} \left(\frac{E(r^k)}{1 + \nu(r^k)} \right) - \dot{\epsilon}_{rr,c} \frac{d}{dr} \left(\frac{E(r)}{1 - \nu(r)^2} \right) \Big|_{r=r^k} \end{aligned} \right] + \left[\begin{aligned} & \frac{\nu(r^k)}{h(r^k)} \frac{dh(r)}{dr} \left(\frac{E(r^k)}{1 - \nu(r^k)^2} \right) \\ & + \frac{1}{r^k} \left(\frac{E(r^k)}{1 + \nu(r^k)} \right) - \nu(r^k) \frac{d}{dr} \left(\frac{E(r)}{1 - \nu(r)^2} \right) \Big|_{r=r^k} \end{aligned} \right] \dot{\epsilon}_{\theta\theta,c} + \left[-\nu(r^k) \left(\frac{E(r^k)}{1 - \nu(r^k)^2} \right) \right] \frac{d\dot{\epsilon}_{rr,c}}{dr} - \left[\left(\frac{E(r^k)}{1 - \nu(r^k)^2} \right) \right] \frac{d\dot{\epsilon}_{\theta\theta,c}}{dr} \tag{19}$$

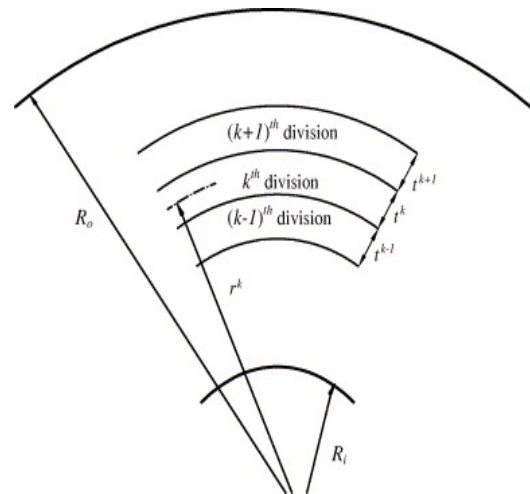


Fig. 2 Dividing radial domain into some finite sub-domains [11]

Also we have:

$$\left(\frac{d\dot{\epsilon}_{rr,c}}{dr} \right)^{k+1} = \frac{(\dot{\epsilon}_{rr,c}^{k+1} - \dot{\epsilon}_{rr,c}^k)}{r^{k+1} - r^k} \tag{20}$$

$$\left(\frac{d\dot{\epsilon}_{\theta\theta,c}}{dr} \right)^{k+1} = \frac{(\dot{\epsilon}_{\theta\theta,c}^{k+1} - \dot{\epsilon}_{\theta\theta,c}^k)}{r^{k+1} - r^k} \tag{21}$$

Using the above technique, Eq. (11) with variable coefficients is changed into a system of m ordinary differential equations with constant coefficients with m being the number of virtual sub-domains.

The solution for Eq. (15) can be written in the form of:

$$\dot{u}_{(r)}^k = X_1^k \exp(\lambda_1^k r) + X_2^k \exp(\lambda_2^k r) - \frac{c_4^k}{c_3^k}; \quad (22)$$

$$r^k - \frac{t^k}{2} \leq r \leq r^k + \frac{t^k}{2}$$

Where X_1^k, X_2^k are unknown constants for kth sub-domain and

$$\lambda_1^k, \lambda_2^k = - \left(\frac{c_2^k \pm \sqrt{(c_2^k)^2 - 4c_1^k c_3^k}}{2c_1^k} \right) \quad (23)$$

The unknowns X_1^k, X_2^k can be determined by applying the necessary conditions between each two adjacent sub-domains. For this purpose, the continuity of the radial displacement rate \dot{u} as well as radial stress rate $\dot{\sigma}_{rr}$ is imposed at the interfaces of the adjacent sub-domains. The continuity conditions at interfaces are given by:

$$\dot{u}_{(r^k+t^k/2)}^k = \dot{u}_{(r^{k+1}-t^{k+1}/2)}^{k+1} \quad (24)$$

$$\dot{\sigma}_{rr}^{k+1} \Big|_{(r=r^k+t^k/2)} = \dot{\sigma}_{rr}^{k+1} \Big|_{(r=r^{k+1}-t^{k+1}/2)} \quad (25)$$

These conditions together with the global boundary conditions of Eq. (12), Eq. (13) or Eq. (14) yield a set of m linear algebraic equations in the form of:

$$[A]_{m \times m} [X]_{m \times 1} = [C]_{m \times 1} \quad (26)$$

$$[X] = [A]^{-1} [C] \quad (27)$$

Solving these equations for X_i^k and substituting them in Eq. (15), the radial displacement rate component, \dot{u} , is determined in each sub-domain. After that we can calculate radial and tangential strain and stress rate by using Eq. (2), Eq. (8), Eq. (9).

6 SOLUTION ALGORITHM

To solve Eq. (11) for FG rotating disks we have these steps:

1. Calculation of thermal distribution over disks
2. Calculation of displacement distribution over disks

3. Calculation of tangential and radial stress and strain distribution using material coefficients for transient analysis

4. Calculation of displacement rate distribution

5. Calculation of tangential and radial stress and strain rate distribution

6. Choosing appropriate time rate $\Delta\tau$ and calculating new stresses and strains. For e.g. for radial stress we have:

$$(\sigma_{rr})_{new} = (\dot{\sigma}_{rr})_{old} \times \Delta\tau + (\sigma_{rr})_{old} \quad (28)$$

7. Repeating the above mentioned 3rd to 6th step until tangential and radial stress and strain rate distribution converge to a constant value

8. Calculation of tangential and radial stress and strain rate distribution using material coefficients for steady state analysis

9. Calculation of tangential and radial displacement distribution for steady state creep

7 NUMERICAL RESULTS

To verify the method presented in this work, at first we compare our results with those of A. Loghman et al [12] and then we continue our discussion about the effects of boundary conditions and other effects on the obtained results.

Now, consider situations assumed in A. Loghman et al [12]. A FG disk with inner radius of 31mm and outer radius of 152.4 mm subjected to 561 K temperature with $\omega = 15000 \text{ rpm}$. The disk was made of a composite, including silicon carbide particles in pure aluminium matrix. Variations of silicon carbide volume fraction along the radius are:

$$C_{(r)} = C_{max} - \left(\frac{r - R_i}{R_o - R_i} \right) (C_{max} - C_{min}) \quad (29)$$

Where $C_{min} = 0.35$ and $C_{max} = 0.104$ are volume fractions of silicon carbide at inner and outer radius respectively. For this investigation the boundary condition is free-free condition.

Fig. 3 and Fig. 4 illustrate rates of radial and tangential strains for disk. As can be observed, results of this work are similar to those of A. Loghman et al [12]. There is a little difference between results due to simplifications of A. Loghman et al [12] in their approach.

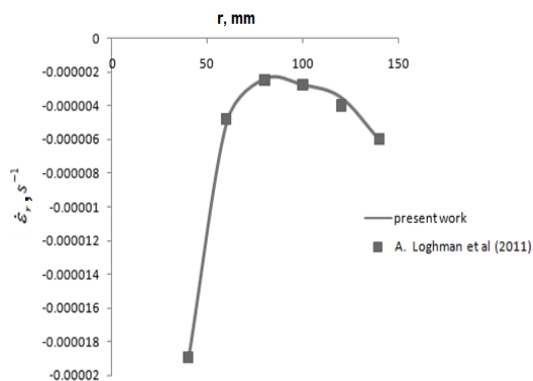


Fig. 3 Radial strain rate comparison of the present work and A. Loghman et al [12]

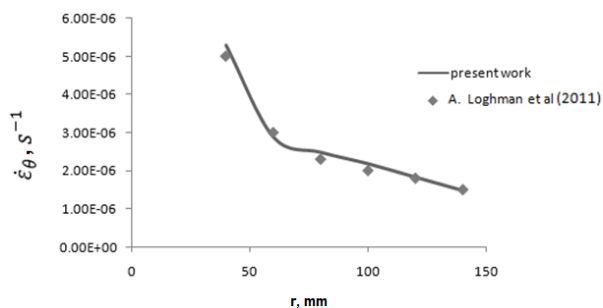


Fig. 4 Tangential strain rate comparison of the present work and A. Loghman et al [12]

Now we examine the effects of some other parameter on the obtained results. We assume FG disk with St 37-2 as its inner surface and zirconium ceramic as its outer surface. Zirconium properties are:

$$\begin{aligned}
 E_{out} &= E_{cer} = 151 \text{ Gpa}, v_{out} = v_{cer} = 0.31, \\
 K_{out} &= K_{cer} = 2j / \text{KgK}, \alpha_{out} = \alpha_{cer} = 10^{-5} / \text{k} \\
 \rho_{out} &= \rho_{cer} = 5700 \text{ Kg} / \text{m}^3
 \end{aligned}
 \tag{30}$$

In Fig. 5, Fig. 6, Fig. 7 and Fig. 8, properties of St 37-2, are presented [10]:

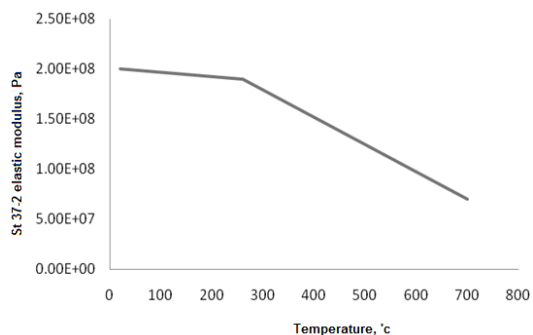


Fig. 5 St 37-2 elastic modulus vs. temperature

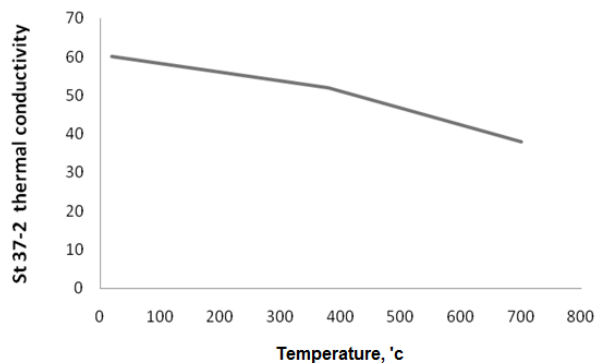


Fig. 6 St 37-2 thermal conductivity vs. temperature

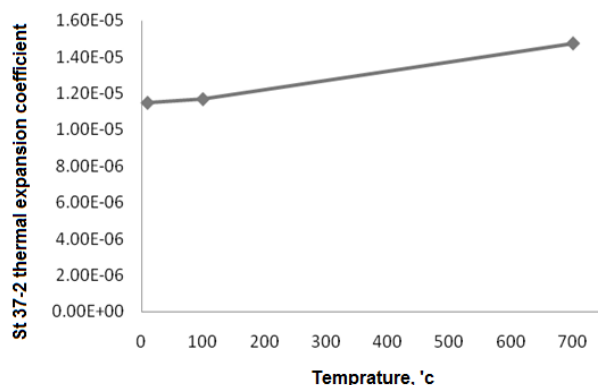


Fig. 7 St 37-2 thermal expansion coefficient vs. temperature

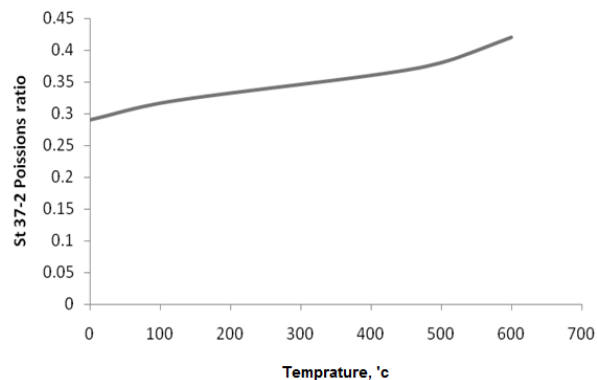


Fig. 8 St 37-2 Poisson ratio vs. temperature

The transient and steady state creep values of Eq. (5), Eq. (6) are:

$$\kappa = 9.9e - 56, \xi = 5.4, q = 0.5 \tag{31}$$

$$\kappa = 5.2e - 56, \xi = 5.4, q = 1 \tag{32}$$

To generalize results, we normalize radial and tangential stresses by dividing them by $\rho_{cer}\omega^2 R_0^2$ and its rate by $\rho_{cer}\omega^2 R_0^2 / E_{cer}$.

In this work disks have inner and outer radius of 15 and 35 centimetres respectively and $\omega = 8000 \text{ rpm}$. Also inner and outer surface temperature of disks is 100 and 500 centigrade degrees. According to Eq. (1) elastic modulus is defined as:

$$E(r) = (E_0 - E_i) \left(\frac{r - r_i}{r_0 - r_i} \right)^n + E_i \quad R_i \leq r \leq R_o \quad (33)$$

where $n = 0.05$ [11].

As shown in Fig. 9, the best thickness profile for variable thickness FG disks is a concave profile [11]:

$$h(r) = 0.019 / r \quad (34)$$

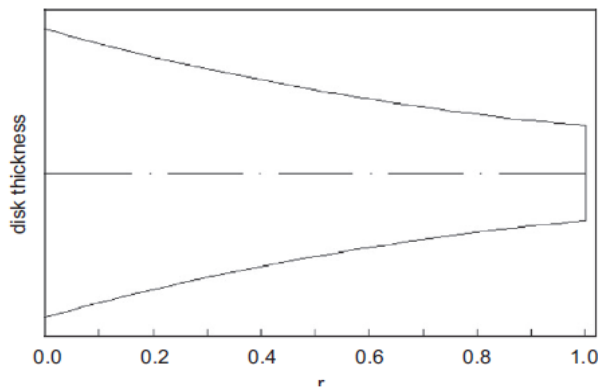


Fig. 9 Disk thickness distribution [11]

8 RESULTS AND DISCUSSION

To check the effects of boundary conditions on steady state creep behaviour of FG disks we suppose 4 types of boundary conditions:

1. Hollow disk free-free:

$$\sigma_{rr} = 0 \text{ at } r = r_i, r = r_o \quad (35)$$

$$\dot{\sigma}_{rr} = 0 \text{ at } r = r_i, r = r_o \quad (36)$$

2. Hollow disk fixed-free:

$$u = 0 \text{ at } r = r_i, \sigma_{rr} = 0 \text{ at } r = r_o \quad (37)$$

$$\dot{u} = 0 \text{ at } r = r_i, \dot{\sigma}_{rr} = 0 \text{ at } r = r_o \quad (38)$$

3. Hollow disk internal pressure-free:

$$\sigma_{rr} = 40 \text{ Mpa at } r = r_i, \sigma_{rr} = 0 \text{ Mpa at } r = r_o \quad (39)$$

$$\dot{\sigma}_{rr} = 0 \text{ at } r = r_i, \dot{\sigma}_{rr} = 0 \text{ Mpa at } r = r_o \quad (40)$$

4. Hollow disk free-External pressure:

$$\sigma_{rr} = 0 \text{ Mpa at } r = r_i, \sigma_{rr} = -40 \text{ Mpa at } r = r_o \quad (41)$$

$$\dot{\sigma}_{rr} = 0 \text{ at } r = r_i, \dot{\sigma}_{rr} = 0 \text{ at } r = r_o \quad (42)$$

Fig. 10 and Fig. 11 illustrate the non-dimensional radial and circumferential strain rate distribution for different boundary conditions after 12 hours from creep beginning. As depicted, strain rate values for fixed-free condition are much higher than those in other boundary conditions.

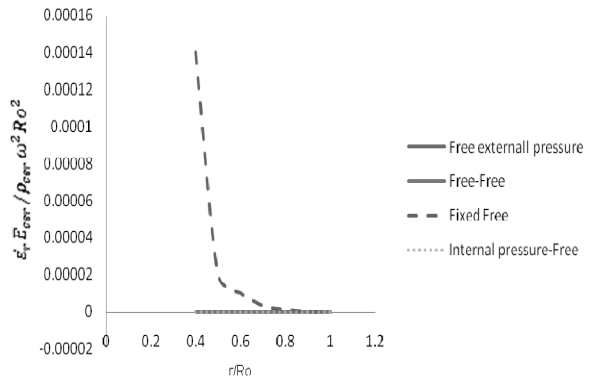


Fig. 10 Non-dimensional radial strain rate distribution for different boundary conditions after 12 hours from creep beginning

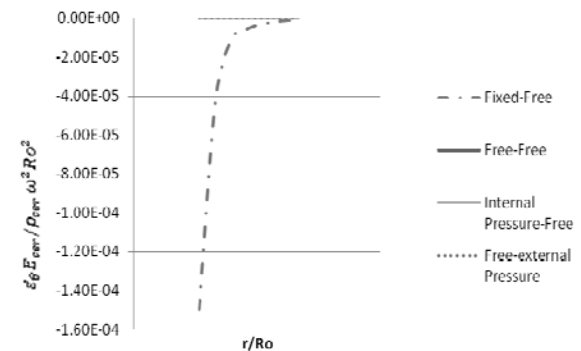


Fig. 11 Non-dimensional circumferential strain rate distribution for different boundary conditions after 12 hours from creep beginning

Fig. 12 and Fig. 13 illustrate the non-dimensional radial and circumferential strain rate distribution for different thermal gradient after 12 hours from creep beginning. As depicted in Fig. 10, radial strain rate begins from positive value and tends to zero along radius and increases with increase in thermal gradient. In Fig. 13 it can be observed that tangential strain rate begins from negative value and tends to zero along radius and increases in negative value with increase in thermal gradient.

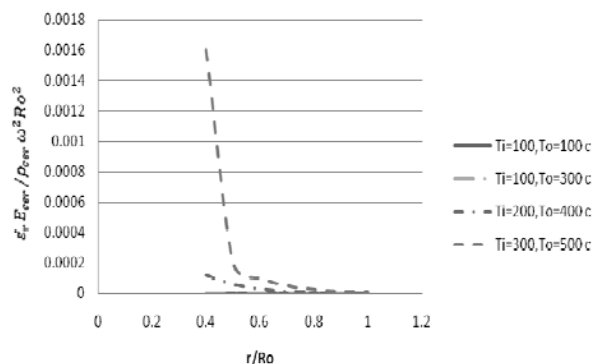


Fig. 12 Non-dimensional radial strain rate distribution for different thermal gradient after 12 hours from creep beginning

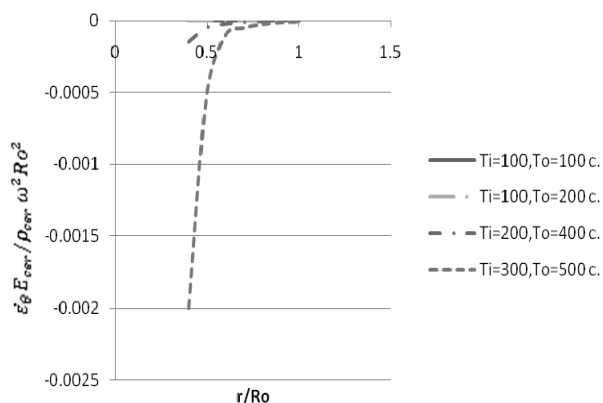


Fig. 13 Non-dimensional tangential strain rate distribution for different thermal gradient after 12 hours from creep beginning

Fig. 14 and Fig. 15 show normalized radial and circumferential stress rate distribution for different thermal gradient after 12 hours from creep beginning. As can be observed, values of stress rate increase when thermal gradient increases.

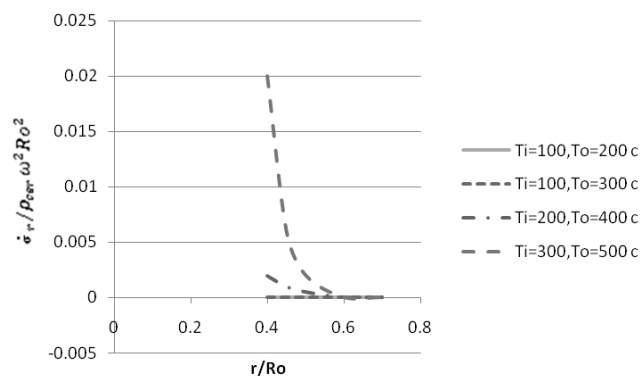


Fig. 14 Non-dimensional radial stress rate distribution for different thermal gradient after 12 hours from creep beginning

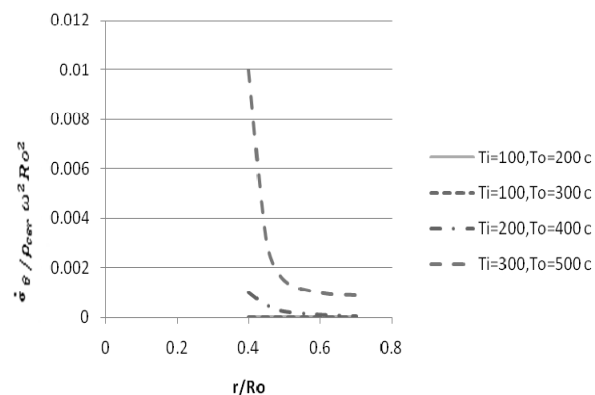


Fig. 15 Non-dimensional circumferential stress rate distribution for different thermal gradient after 12 hours from creep beginning

9 CONCLUSION

In this article, a semi-analytical solution of time-dependent creep analysis of rotating thin disk made of FG materials is examined. Displacement equation and steady state creep equation for the disk were derived using the thermo-elastic theory and Norton's principle respectively. To solve these equations, the disk is divided into virtual sub-domains. Equilibrium equations in each sub-domain are ordinary differential equations with constant coefficients whose general solution can be obtained by imposing the continuity conditions at the interface of the adjacent sub-domains together with global conditions. Also some case studies and verifications were examined to show the accuracy of the presented method. Some general observations of this study can be summarized as follows:

- The best creep behaviour of FG disks belongs to fixed-free boundary condition. This condition is also the most practical condition.
- Thermal dependency of metal properties used in the disk, increases stresses and strains. Notice that neglecting this dependency causes glaring errors in analysing FG disks that might not compensate with low safety factors.
- It is important to choose appropriate boundary conditions during mounting of FG disks. This is because of the dependency of FG disks behaviour to boundary conditions.
- The stress and strain rates of creep values differ from high to low values along radius. These high values are not good criterions to judge.
- Creep stress and strains increase with increasing thermal gradient.

REFERENCES

- [1] Yang, Y. Y., "Time-dependent Stress Analysis in Functionally Graded Materials", *Solids and Structures*, Vol. 37, No. 2, 2000, pp. 7593-7608.
- [2] Singh, S. B. and Ray, S., "Modeling the Anisotropy and Creep in Orthotropic Aluminum-silicon Carbide Composite Rotating Disc", *Mechanics of Materials*, Vol. 34, No. 2, 2002, pp. 363-372.
- [3] Liew, K. M., Kitipornchai, S., Zhang, X. Z. and Lim, C. W., "Analysis of the Thermal Stress Behavior of Functionally Graded Hollow Circular Cylinders", *Solids and Structures*, Vol. 40, No. 5, 2003, pp. 2355-2380.
- [4] Singh, S. B. and Ray, S., "Creep Analysis in an Isotropic FGM Rotating Disc of Al-SiC Composite", *Materials Processing Technology*, Vol. 143-144, 2003, pp. 616-622.
- [5] Eslami, M. R., Babaei, M. H. and Poultangari, R., "Thermal and Mechanical Stresses in a Functionally Graded Thick Sphere", *Pressure Vessels and Piping*, Vol. 82, 2005, pp. 522-527.
- [6] Hosseini Kordkheili, S. A. and Naghdabadi, R., "Thermoelastic analysis of functionally graded rotating disk", *Composite Structures*, Vol. 79, 2007, pp. 508-516.
- [7] Farshi, B. and Bidabadi, J., "Optimum Design of Inhomogeneous Rotating Discs under Secondary Creep", *Pressure Vessels and Piping*, Vol. 85, 2008, pp. 507-515.
- [8] Singh, S. B., "One Parameter Model for Creep in a Whisker Reinforced Anisotropic Rotating Disc of Al-SiC Composite", *Mechanics of Solids*, Vol. 27, 2008, pp. 680-690.
- [9] Poultangari, R., Jabbari, M. and Eslami, M. R., "Functionally Graded Hollow Spheres under Non-axisymmetric Thermo-mechanical Loads", *Pressure Vessels and Piping*, Vol. 85, 2008, pp. 295-305.
- [10] Pankaj and Sonia, R. Bansal, "Creep Transition in a Thin Rotating Disk Having Variable Density with Inclusion", *Engineering and Technology*, Vol. 28, 2008, pp. 2070-3740.
- [11] Bayat, M., Saleem, M., Sahari, B., Hamouda, A. M. S. and Mahdi, E., "Mechanical and Thermal Stresses in a Functionally Graded Rotating Disk with Variable Thickness due to Radially Symmetry Loads" *Pressure Vessels and Piping*, Vol. 86, Issue 6, 2009, pp. 357-372.
- [12] Loghman, A., Ghorbanpour Arani, A., Shajari, A. R. and Amir, S., "Time-dependent Thermoelastic Creep Analysis of Rotating Disk Made of AL-SiC Composite", *Archive of Applied Mechanics*, Vol. 81, 2009, pp.1853-1864, 2011.